Chemical Inhomogeneity and Mixed-State Ferromagnetism in Diluted Magnetic Semiconductor Co:TiO_2

Satishchandra Ogale,*[,†] Darshan Kundaliya,[‡] Shareghe Mehraeen,[§] Lian-feng Fu,[§] Shixiong Zhang,[‡] Alexandre Lussier,[¶] Joe Dvorak,[¶] Nigel Browning,[§] Yves Idzerda,[¶] and Thirumalai Venkatesan[‡,$]

Physical and Materials Chemistry Division, National Chemical Laboratory, Dr. Homi Bhabha Road, Pune-411008, India, Center for Superconductivity Research, Department of Physics, University of Maryland, College Park, Maryland 20742-4111, Department of Chemical Engineering and Materials Science, University of California-Davis, One Shields Avenue, Davis, California 95616, National Center for Electron Microscopy, MS 72–150, Lawrence Berkeley National Laboratory, Berkeley, California 94720, Department of Physics, Montana State University, Bozeman, Montana 59717, and National University of Singapore, 21 Lower Kent Ridge Road, Singapore 119077

Received July 30, 2007. Revised Manuscript Received November 27, 2007

Diluted magnetic semiconductors (DMS) are among the most intensely investigated materials in recent times in view of their great application potential. Yet, they are also the most controversial because of the possibility of extrinsic effects attributable to dopant solubility and clustering, point defects, incorporation of unintentional impurities, etc. This has highlighted the central role of materials chemistry in rendering a specific microstate and property response. In this work, we provide a combined window of high-resolution scanning transmission electron microscopy and electron energy-loss spectrometry, X-ray absorption (XAS)/X-ray magnetic circular dichroism (XMCD), and magnetization measurements on epitaxial rutile $Co_xTi_{1-x}O_2$ ($x = 0$–0.06) system (the first discovered oxide-DMS, which continues to be controversial) grown at low temperature (400 °C) under different ambient atmospheres. The study brings out a mixed-state scenario of ferromagnetism involving intrinsic DMS (uniform dopant distribution at low dopant concentration) and coupled cluster magnetism, involving cobalt associations within the matrix at higher concentrations. We also show that by matrix valence control during growth, it is possible to realize a uniform embedded cluster state and the related coupled cluster magnetism.

Introduction

Semiconducting matrices dilutely doped with magnetic impurities have been the focus of intense scientific activity for the past several years.[1–10] Such materials, termed as diluted magnetic semiconductors (DMS), if realized in homogeneous form without extrinsic undesirable phases, are projected to have significant implications for the evolving fields of spintronics and advanced magneto-optics. Such materials are also viewed as breeding grounds for potentially new mechanisms of magnetic interactions.[11–19] Interestingly, ferromagnetism has been suggested to be possible even without magnetic dopant inclusion.[14,15,18–20] Unfortunately however, except for a couple of favorable cases of materials systems, the promise of the field appears to have been clouded by materials issues arising from questions about dopant uniformity, defect states, and secondary phases. This has been particularly the case with most oxide-based DMS systems, such as transition element (in particular Co, Mn)

* Corresponding author. Fax: 91-20-25902636. Phone: 91-20-25902260. E-mail: sb.ogale@ncl.res.in.
† National Chemical Laboratory.
‡ University of Maryland.
§ University of California-Davis and Lawrence Berkeley National Laboratory.
¶ Montana State University.
$ National University of Singapore.

(1) Ohno, H. *Science* **1998**, *281*, 951.
(2) Dietl, T.; Ohno, H.; Matsukura, F.; Cibert, J.; Ferrand, D. *Science* **2000**, *287*, 1019.
(3) Zutic, I.; Fabian, J.; Das Sarma, S. *Rev. Mod. Phys.* **2004**, *76*, 323.
(4) Coey, J. M. D. *Curr. Opin. Solid State Mater.Sci.* **2006**, *10*, 83.
(5) Dietl, T.; Ohno, H. *Mater. Today* **2006**, *9*, 18.
(6) Chambers, S. A.; Droubay, T. C.; Wang, C. M.; Rosso, K. M.; Heald, S. M.; Schwartz, D. A.; Kittilstved, K. R.; Gamelin, D. R. *Mater. Today* **2006**, *9*, 28.
(7) Macdonald, A. H.; Schiffer, P.; Samarth, N. *Nat. Mater.* **2005**, *4*, 195.
(8) Awschalom, D. D.; Flatte, M. *Nat. Phys.* **2007**, *3*, 153.
(9) Wolf, S. A.; Awschalom, D. D.; Buhrman, R. A.; Daughton, J. M.; von Molnar, S.; Roukes, M. L.; Chtchelkanova, A. Y.; Treger, D. M. *Science* **2001**, *294*, 1488.
(10) Ogale, S. B. *Thin Films and Heterostructures for Oxide Electronics* Springer Verlag, Berlin, 2005.
(11) Kaminski, A.; Das Sarma, S. *Phys. Rev. Lett.* **2002**, *88*, 247202.
(12) Coey, J. M. D.; Venkatesan, M.; Fitzgerald, C. B. *Nat. Mater.* **2005**, *4*, 173.
(13) Konig, J.; Lin, H. H.; MacDonald, A. H. *Phys. Rev. Lett.* **2000**, *84*, 5628.
(14) Elfimov, I. S.; Yunoki, S.; Sawatzky, G. A. *Phys. Rev. Lett.* **2002**, *89*, 216403.
(15) Osorio-Guillen, J.; Lany, S.; Barabash, S. V.; Zunger, A. *Phys. Rev. Lett.* **2006**, *96* (10), 107203.
(16) Priour, D. J.; Das Sarma, S. *Phys. Rev. Lett.* **2006**, *97*, 127201.
(17) Popescu, F.; Yildirim, Y.; Alvarez, G.; Moreo, A.; Dagotto, E. *Phys.Rev. B* **2006**, *73*, 075206.
(18) Venkatesan, M.; Fitzgerald, C. B.; Coey, J. M. D. *Nature* **2004**, *430*, 630.
(19) Elfimov, I. S.; Rusydi, A.; Csiszar, S. I.; Hu, Z.; Hsieh, H. H.; Lin, H.-J.; Chen, C. T.; Liang, R.; Sawatzky, G. A. *Phys. Rev. Lett.* **2007**, *98*, 137202.
(20) Sundaresan, A.; Bhargavi, R.; Rangarajan, N.; Siddesh, U.; Rao, C. N. R. *Phys. Rev. B.* **2006**, *74*, 161306.
(21) Matsumoto, Y.; Murakami, M.; Shono, T.; Hasegawa, T.; Fukumura, T.; Kawasaki, M.; Ahmet, P.; Chikyow, T.; Koshihara, S.; Koinuma, H. *Science* **2001**, *291*, 854.

10.1021/cm702089z CCC: $40.75
Published on Web 01/17/2008

doped TiO_2,[21–30] ZnO,[31–38] SnO_2,[39] $La_{1-x}Sr_xTiO_3$,[40,41] etc., because oxygen nonstoichiometry during materials synthesis sensitively affects the microstate, including dopant clustering and defect formation. In spite of significant efforts expended on elucidating the nature of microstates by various techniques and their relationship to the observed magnetism, these questions have remained largely unresolved. It has therefore become necessary to probe such materials using even finer elemental and element specific probes for ascertaining the chemical character and uniformity of dopants. In a very recent study by Dietl and co-workers[42] on the (Zn,Cr)Te system, the significance of elemental mapping and microanalyses is emphasized and shown to provide new insights into the attendant issues and possibly a new direction for controlled DMS synthesis. Indeed, as Samarth has pointed out,[43] ferromagnetic clusters may not necessarily be a negative for DMS science if they can be suitably tailored. In this work, we examine the issues of dopant uniformity, clustering, and possible cluster manipulation in the case of the Co:TiO_2 system, which was the first oxide DMS to be discovered by Matsumoto et al.,[21] the most investigated by several groups, and yet continues to be controversial. We provide a combined window of high-resolution scanning transmission electron microscopy and electron energy-loss spectrometry, X-ray absorption (XAS)/X-ray magnetic circular dichroism (XMCD), and magnetization measurements on epitaxial rutile $Co_xTi_{1-x}O_2$ ($x = 0$–0.06) system grown at low temperature (400 °C) under different atmospheric conditions, to reveal a mixed-state scenario involving intrinsic DMS (at low dopant concentration) and coupled cluster magnetism involving cobalt associations within the matrix at higher associations. We also show that by matrix valence control during growth, it is possible to realize a uniform embedded cluster state and the related coupled cluster magnetism. This conforms to the idea promoted by Dietl and co-workers.[42]

The cobalt-doped TiO_2 system has been synthesized by various methods in different forms and phases (rutile vs anatase) over different ranges of temperature and pressure parameters.[6,21–25,27–30] In most instances, high-temperature processing has been found to lead to some form of dopant clustering.[6,25,27] Therefore, in this work, we have resorted to growth at relatively low temperature of 400 °C.[21] We have also controlled the ambient type and pressure to examine the evolution of the microstate and have concurrently examined the physical properties. It appears that the Co:TiO_2 system is susceptible to formation of tiny cobalt clusters (not necessarily metallic cobalt clusters) even at low temperature beyond some level of solubility. The apparent ferromagnetism in such a mixed phase may represent an interesting condition wherein the partially dissolved substitutional cobalt phase may act as exchange glue for magnetic ordering of the rest of the superparamagnetic clusters.

Experimental Section

A pulsed laser deposition (PLD) technique was used to deposit thin films. The Co-doped TiO_2 targets (discs of diameter ~20 cm and thickness 3–5 mm) were prepared by a solid-state reaction method that included multiple grinding/mixing and high-temperature (~1175 °C) heating and sintering steps. Using such targets, thin films were PLD grown at low temperature (400 °C) onto R-Al_2O_3 single-crystal substrates at different oxygen and Ar + H_2 partial pressures (400 mTorr down to $<1 \times 10^{-6}$ Torr). X-ray diffraction technique (Siemens D5000) was used to check the structure and phase of the films and the lattice change due to incorporation of the transition metal. Magnetization measurements were carried out using a SQUID magnetometer (MPMS XL, Quantum Design, USA). X-ray absorption spectroscopy (XAS) was used to identify the substitutional nature of cobalt atoms in the TiO_2 matrix as well as the corresponding valence state and the valence state of the matrix (Ti edge). The measurements were made at the MSU X-ray Nanomaterials Characterization Facility located at beamline U4-B of the National Synchrotron Light Source (NSLS), and at Beamline 4.0.2 at the Advanced Light Source (ALS). The Z-contrast scanning transmission electron microscopy (STEM) and electron energy-loss spectroscopy (EELS) experiments were carried out using a Schottky field-emission gun (FEG) FEI Tecnai F20UT microscope operated at 200 kV with a spatial resolution of 0.14 nm in scanning electron transmission mode (0.4 nm for EELS) and an energy resolution of 0.5 eV. High-quality cross-section electron microscopy samples were prepared using the shadow technique, a sample preparation technique that combines a small-angle cleavage technique with

(22) Weng, H. M.; Dong, J. M.; Fukumura, T.; Kawasaki, M.; Kawazoe, Y. *Phys. Rev. B* **2006**, *73*, 121201.
(23) Weng, H. M.; Yang, X. P.; Dong, Mizuseki, H.; Kawasaki, M.; Kawazoe, Y. *Phys. Rev. B* **2004**, *69*, 125219.
(24) Quilty, J. W.; Shibata, A.; Son, J. -Y.; Takubo, K.; Mizokawa, T.; Toyosaki, H.; Fukumura, T.; Kawasaki, M. *Phys. Rev. Lett.* **2006**, *96*, 027202.
(25) Kim, J.-Y.; Park, J.-H.; Park, B.-G.; Noh, H.-J.; Oh, S.-J.; Yang, J. S.; Kim, D.-H.; Bu, S. D.; Noh, T.-W.; Lin, H.-J.; Hsieh, H.-H.; Chen, C. T. *Phys. Rev. Lett.* **2003**, *90*, 017401.
(26) Zhao, T.; Shinde, S. R.; Ogale, S. B.; Zheng, H.; Venkatesan, T.; Ramesh, R.; Das Sarma, S. *Phys. Rev. Lett.* **2005**, *94*, 126601.
(27) Shinde, S. R.; Ogale, S. B.; Higgins, J. S.; Zheng, H.; Millis, A. J.; Kulkarni, V. N.; Ramesh, R.; Greene, R.; Venkatesan, T. *Phys. Rev. Lett.* **2004**, *92*, 166601.
(28) Griffin, K. A.; Pakhomov, A. B.; Wang, C. M.; Heald, S. M.; Krishnan, K. M. *Phys. Rev. Lett.* **2005**, *94*, 157204.
(29) Toyosaki, H.; Fukumura, T.; Yamada, Y.; Nakajima, K.; Chikyow, T.; Hasegawa, T.; Koinuma, H.; Kawasaki, M. *Nat. Mater.* **2004**, *3*, 221.
(30) Bryan, J. D.; Heald, S. M.; Chambers, S. A.; Gamelin, D. R. *J. Am. Chem. Soc.* **2004**, *126*, 11640.
(31) Kundaliya, D. C.; Ogale, S. B.; Lofland, S. E.; Dhar, S.; Metting, C. J.; Shinde, S. R.; Ma, Z.; Verughese, B.; Ramanujachary, K. V.; Salamanca-Riba, L.; Venkatesan, T. *Nat. Mater.* **2004**, *3*, 709.
(32) Sluiter, M. H. F.; Kawazoe, Y.; Sharma, P.; Inoue, A.; Raju, A. R.; Rout, C. U. V.; Waghmare, U. V. *Phys. Rev. Lett.* **2005**, *94*, 187204.
(33) Kittilstved, K. R.; Schwartz, D. A.; Tuan, A. C.; Heald, S.M.; Chambers, S. A.; Gamelin, D. R. *Phys. Rev. Lett.* **2006**, *97*, 037203.
(34) Venkatesan, M.; Fitzgerald, C. B.; Lunney, J. G.; Coey, J. M.D. *Phys. Rev. Lett.* **2004**, *93*, 177206.
(35) Kittilstved, K. R.; Liu, W. K.; Gamelin, D. R. *Nat. Mater.* **2006**, *5*, 291.
(36) Jayakumar, O. D.; Gopalakrishnan, I.; Kulshreshtha, S. K. *Adv. Mater.* **2006**, *18*, 1857.
(37) Wang, X. F.; Xu, J. B.; Zhang, B.; Yu, H. G.; Wang, J.; Zhang, X. X.; Yu, J. G.; Li, Q. *Adv. Mater.* **2006**, *18*, 2476.
(38) Schwartz, D. A.; Gamelin, D. R. *Adv. Mater.* **2004**, *16*, 2115.
(39) Ogale, S. B.; Choudhary, R. J.; Buban, J. P.; Lofland, S. E.; Shinde, S. R.; Kale, S. N.; Kulkarni, V. N.; Higgins, J.; Lanci, C.; Simpson, J. R.; Browning, N. D.; Das Sarma, S.; Drew, H. D.; Greene, R. L.; Venkatesan, T. *Phys. Rev. Lett.* **2003**, *91*, 077205–1.
(40) Zhao, Y. G.; Shinde, S. R.; Ogale, S. B.; Higgins, J.; Choudhary, R. J.; Kulkarni, V. N.; Greene, R. L.; Venkatesan, T.; Lofland, S.; Lanci, C.; Buban, J.; Browning, N. D.; Das Sarma, S.; Millis, A. *J. Appl. Phys. Lett.* **2003**, *83*, 2199.
(41) Herranz, G.; Ranchal, R.; Bibes, M.; Jaffres, H.; Jacquet, E.; Maurice, J. L.; Bouzehouane, K.; Wyczisk, F.; Tafra, E.; Basletic, M.; Hamzic, A.; Colliex, C.; Contour, J. P.; Barthelemy, A.; Fert, A. *Phys. Rev. Lett.* **2006**, *96*, 027207.
(42) Kuroda, S.; Nishizawa, N.; Takita, K.; Mitome, M.; Bando, Y.; Osuch, Dietl, T. *Nat. Mater.* **2007**, *6*, 440.
(43) Samarth, N. *Nat. Mater.* **2007**, *6*, 403.

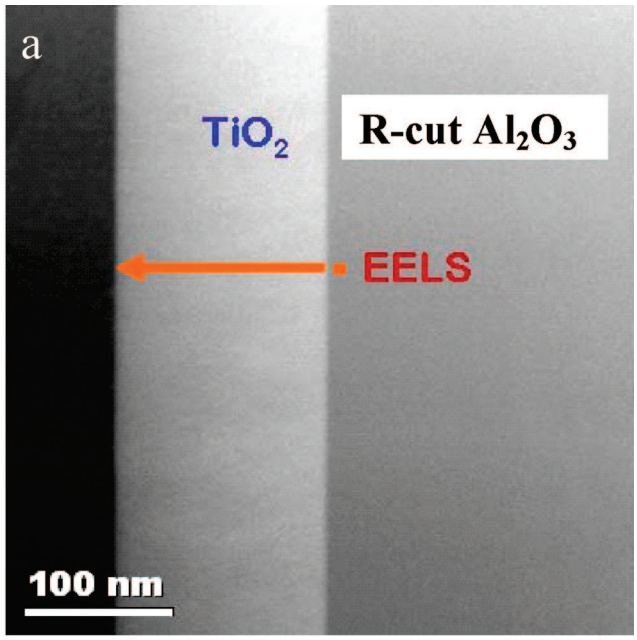

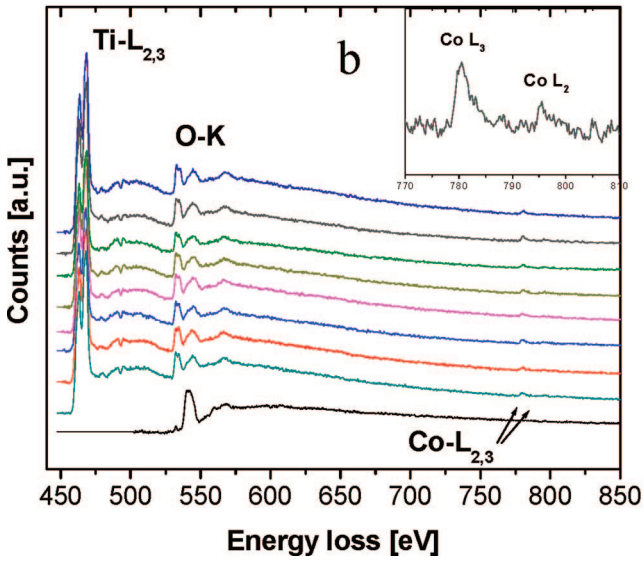

Figure 1. (a) High-resolution cross-section HAADF STEM image for a $Co_xTi_{1-x}O_2$ film with $x = 0.04$ grown at 400 °C in a vacuum greater than 1×10^{-6} Torr, (b) EELS data recorded at various points across the film cross-section. Inset shows details for Co-$L_{2,3}$ for a typical case.

focused ion beam (FIB), minimizing sample modification. Core-loss EEL spectra were recorded with dispersions of 0.2 eV/channel and the exposure time was limited to 6 s to avoid beam damage. The background for each core-loss spectrum was subtracted by a power-law fitting method.

Results and Discussion

In Figure 1a, we show the high-resolution cross-section HAADF STEM image for a $Co_xTi_{1-x}O_2$ film with $x = 0.04$ grown at 400 °C in a vacuum better than 1×10^{-6} Torr. It can be immediately seen that this film is very homogeneous throughout the cross-section without any sign of apparent cobalt clusters or other structural inhomogeneities. This is in stark contrast to the various cases of high temperature depositions discussed in the literature, wherein some form

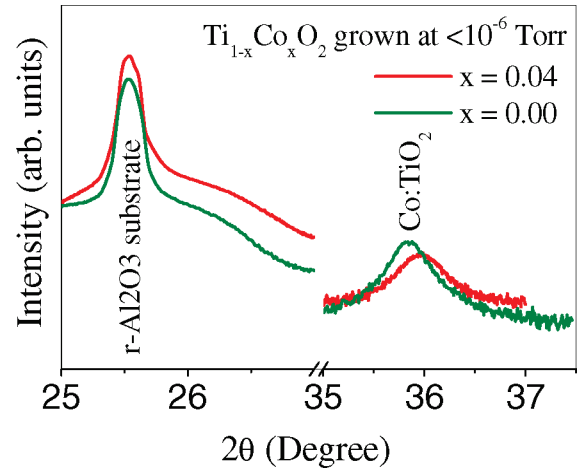

Figure 2. X-ray diffraction data (main rutile peak) for the undoped and $x = 0.04$ cobalt-doped TiO_2 films grown at 400 °C under a vacuum greater than 1×10^{-6} Torr.

of clustering is apparent especially at concentrations higher than about $x = 0.02$. The results of EELS studies performed with a resolution of ~0.4 nm at various points across the cross-section (0.14 nm STEM resolution) are compiled in Figure 1b. The Ti-$L_{2,3}$ and O-K edges (when analyzed in detail) reflect the rutile phase, as was verified from the X-ray diffraction data. Importantly, the cobalt L_2, L_3 signal is found to be highly uniform across the cross-section, suggesting that cobalt is dispersed fairly uniformly in the film. Thus, just on the basis of these data, one may conclude that under this growth condition, one would get an intrinsic DMS system. As we discuss later, other measurements, however, need to be done before the conclusion can be solidified.

In Figure 2, we compare the X-ray diffraction data (main rutile peak) for the undoped and $x = 0.04$ cobalt-doped TiO_2 films grown at 400 °C under a vacuum better than 1×10^{-6} Torr.

As can be seen the main substrate, peak positions overlap completely (normalization). The main rutile peak shows an unambiguous shift to higher 2θ or lower out-of-plane d value upon cobalt doping. This suggests that the doped film is under slight tensile strain as compared to the undoped one, implying smaller lattice parameter. Substitution of cobalt with its 2+ valence (ionic radius 75 p.m.) for Ti 4+ (ionic radius 61 p.m.) generates an oxygen vacancy for local charge balance, and these together can lead to such a lattice parameter change. Thus, a shift in XRD peak position indicates that some cobalt has gone substitutionally in the matrix.

The room temperature M vs H data for the $Co_xTi_{1-x}O_2$ films ($x = 0.0$–0.06) grown at 400 °C under a vacuum better than 1×10^{-6} Torr are shown in Figure 3a. The field-cooled (FC) and zero-field-cooled (ZFC) data for the case of the $x = 0.04$ sample are shown in Figure 3b. From Figure 3a it can be seen that all of these curves show nonlinear behavior with a low coercivity. The coercive field (insets) is higher (~100 Oe) for $x = 0.0025$, whereas it is somewhat lower (75 Oe) for $x = 0.04$. The saturation magnetization increases with increasing cobalt concentration, but the increase between $x = 0.02$ and $x = 0.04$ is quite sharp and substantial, suggesting the possibility of formation of cobalt clusters above about $x = 0.02$ concentration, as discussed below.

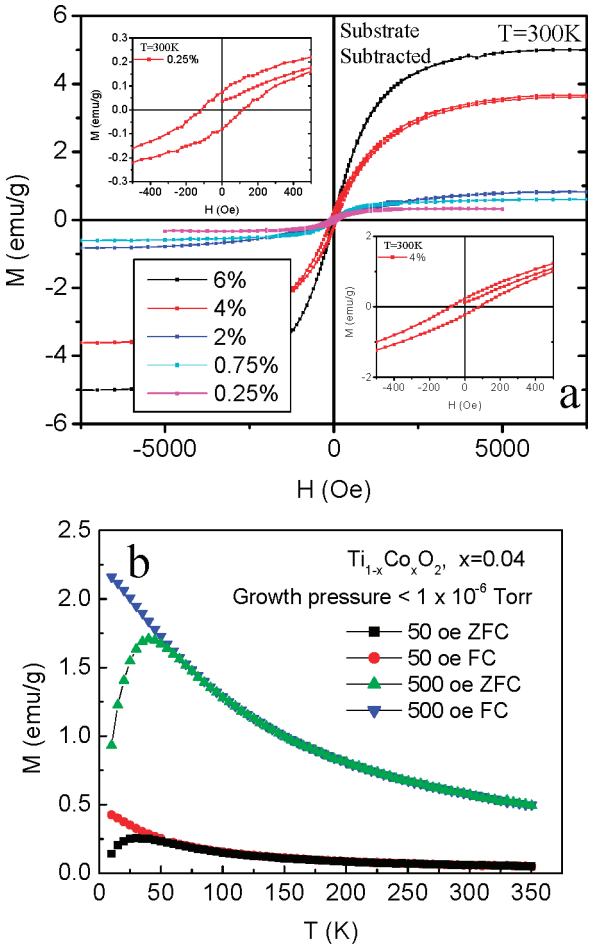

Figure 3. (a) Room-temperature M vs H data for the $Co_xTi_{1-x}O_2$ films (x = 0.0–0.06) grown at 400 °C under vacuum of better than 1 × 10^{-6} Torr, (b) field-cooled (FC) and zero-field-cooled (ZFC) magnetization for the case of the x = 0.04 sample.

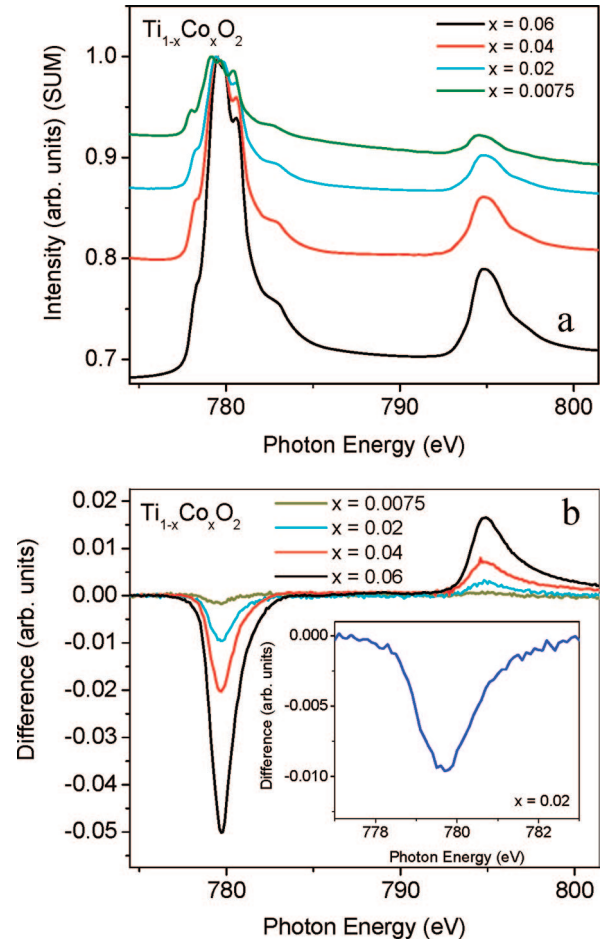

Figure 4. (a) X-ray absorption (XAS) and (b) X-ray magnetic circular dichroism (X-MCD) data for some $Co_xTi_{1-x}O_2$films (x = 0.0–0.06) grown at 400 °C under a vacuum greater than 1 × 10^{-6} Torr.

From Figure 3b, the FC magnetization is seen to decrease monotonically during warming at both fields (50 Oe, 500 Oe), while the ZFC magnetization is seen to increase up to a temperature T_B and then decrease upon further warming. This behavior indicates superparamagnetic nature of this system. The temperature $T_B \approx 30$ K, where the low magnetic field ZFC magnetization peak locates, is the so-called blocking temperature. We can calculate the size of these clusters by the formula: $K_AV = 25k_BT_B$, where K_A is the magnetic anisotropy constant and k_B is the Boltzmann constant. Nominally using $K_A \approx 4.5 \times 10^6$ ergs/cm^3 for cobalt metal, the mean cluster size of $V \approx 21.7$ nm^3 (or a mean cluster diameter of $D \approx 3.2$ nm) can be inferred. One should remember, however, that this is just an estimate assuming that they could be cobalt metal clusters, but the clusters may simply be substitutional cobalt clusters and then the corresponding parameters could be different. Indeed, as discussed later, theoretical studies do predict substitutional cobalt associations in the matrix under certain growth conditions and these are also ferromagnetic. Considering the cobalt uniformity observed in the HAADF STEM and the relaxation of lattice parameter signifying substitutional incorporation of cobalt, this result is rather surprising. Because the magnetization measurements are intrinsically cumulative over large sample, the observed superparamagnetic effects imply that some cobalt clusters could be present in some dilutely distributed regions near the surface or interface. Toward this end, we asked ourselves a question whether the observed cobalt uniformity in Figure 1is due to the fact that the sample is not milled enough and is thick with overlapping nonuniformity, leading to apparent uniformity. To examine this, we milled the sample much further and examined it in cross-section. The corresponding data shown in the Supporting Information revealed nonuniformity of cobalt distribution as seen from the contrast distribution. Given the fact that sapphire substrate is hard to ion mill, this state of the sample is subjected to significant radiation and a lingering question would remain whether the observed inhomogeneity is itself caused by heavy milling. Nonetheless, a remarkable thing to note from the Supporting Information is that the high-contrast regions have the same structure as rutile TiO_2. This would imply the presence of subsitutional cobalt redistribution within the sample and by implication cobalt associations within the matrix rather than cobalt metal clusters. The EDAX data revealed the mean concentration of about 4%, as expected.

In Figure 4, we show the X-ray absorption (XAS) and X-ray magnetic circular dichroism (XMCD) data for some $Co_xTi_{1-x}O_2$ films (x = 0.0–0.06) grown at 400 °C under a vacuum better than 1 × 10^{-6} Torr. It should be remembered that this information emanates only from the top 5–10 nm

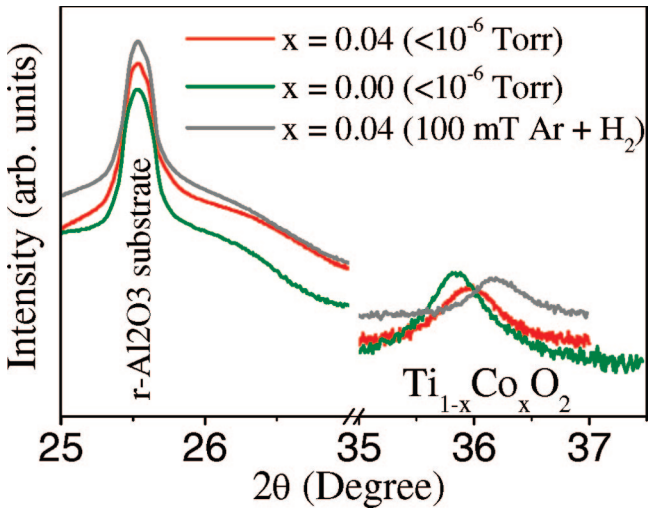

Figure 5. X-ray diffraction data (main TiO_2 peak and substrate peak) for a $Co_{0.04}Ti_{0.96}O_2$ film grown at 400 °C at 100 mTorr of Ar + H_2, compared to the corresponding data for the undoped and $x = 0.04$ films grown in a vacuum greater than 1×10^{-6} Torr.

region near the sample surface; hence, what is being reflected in these data does not pertain to the whole cross-section of the sample. Although the fine structures noted on the XAS features tend to suggest the presence of Co^{2+} implying full substitution, the presence of a featureless component signifying Co(0) can not be ruled out just from the L-edge XAS data. The XMCD (difference) spectra, shown in Figure 4b, appear featureless, especially for higher concentrations.

At concentrations $x = 0.02$ and lower, the fine structures are present (inset), although they are less pronounced than in the XAS data. This would imply that at least in the surface regions, one may have cobalt clusters, more so at concentrations higher than about $x = 0.02$. That such clusters are not observed in the HAADF STEM data of Figure 1a suggests that these may be planar clusters. It must be emphasized on the basis of a fairly uniform cobalt signal seen across the cross-section in Figure 1b that such clusters do not represent the whole sample. On the basis of all this collective evidence, it seems that such films are intrinsic DMS systems, but not completely free for cobalt clusters, at least at concentrations higher than $x = 0.02$. It is tempting to suggest that at higher cobalt concentrations, the intrinsic DMS ferromagnetism of the dilutely dispersed system may act as an exchange glue coupling the distributed cobalt clusters, rendering the whole sample ferromagnetic with an enhanced moment. We will return to this matter once again later.

In an attempt to explore the behavior of the system under differing reducing conditions involving hydrogen rather than depleted oxygen, as in the case of vacuum grown films, we grew some film samples in Ar + H_2 ambient gas. Another objective of this study was to explore the possibility of stabilizing interesting microstates in the same system with hydrogen, which is known to play peculiar role in inorganic solids. In Figure 5 are shown the XRD data (main TiO_2 peak with the substrate peak) for a $Co_{0.04}Ti_{0.96}O_2$ film grown at 400 °C at 100 mTorr of Ar + H_2, and the same are compared with the data for the undoped and $x = 0.04$ films grown in a vacuum as discussed in the previous sections. Note the normalization of the substrate position for all cases. A remarkable shift is seen in the main TiO_2 peak for the film grown in Ar + H_2 as compared to the other cases, which suggests a significant change in the state of the sample under this new growth condition, inviting microscopic analyses, which we discuss next.

In Figure 6a, we show the HAADF STEM data for the Ar + H_2 grown film. This sample clearly shows enhanced nanoscale contrast inhomogeneity, distinctly different from the rather uniform HAADF STEM image of Figure 1a for the vacuum-grown case. Because the contrast in the HAADF STEM is a signature of elemental Z value, the observed inhomogeneity suggests dopant distribution inhomogeneity.

As can be noted from the EELS data across the sample (Figure 6b), the cobalt signal is seen to fluctuate rather substantially across the cross-section. To elucidate the inhomogeneity aspect still further, we focused our attention on a few apparent white nanodots in the image and found unmistakable cobalt signal in each such location (panels c and d in Figure 6). This implies that one does get cobalt clusters under the new Ar + H_2 condition employed.

The details shown as insets do not reveal any significant differences at the three locations. Once again, whether these are cobalt metal clusters or cobalt substitutional clusters needs separate consideration, as discussed later.

It is interesting that the tiny clusters are embedded rather uniformly across the cross-section, rather than getting dispensed at the interface or surface as was observed in some earlier works. This may be an interesting route for the synthesis of nanoengineered functional materials with self-assembled bulk distributed magnetic nanodots (as very recently emphasized by Dietl and co-workers[42] and Samarth[43]), which in the case of magnetic materials may be of interest for applications involving magneto-optic Faraday rotation effects.

In Figure 7a, we show the FC and ZFC magnetization dependence on temperature of a $Co_{0.04}Ti_{0.96}O_2$ film grown at 400 °C and 100 mTorr of Ar + H_2, whereas in Figure 7b, we show the room-temperature $M-H$ loop for the same case. A superparamagnetic-like behavior is clearly observed with the blocking temperature of ~40 K (we term this superparamagnetic-like because, as shown and discussed next, a finite coercive field is observed in this case above the stated blocking temperature). The cluster size is found to be ~30 nm^3, slightly larger than those in the film grown in a vacuum. The main and dramatic difference, however, between the two cases of ambient growth is that in the Ar + H_2 case, we see most cobalt in the form of distributed clusters, whereas in vacuum-grown films, no clear clusters are seen.

From the $M-H$ data at 300 K, the coercive field is about 120 Oe, and the saturated magnetization is 1.2 emu/g, which is much lower than the same of the film grown in a vacuum (which was >3 emu/g). The appearance of finite coercive field at 300 K (above the blocking temperature) possibly implies coupled cluster magnetism and the lower moment should imply imperfect magnetic order. With reference to the earlier argument, with most cobalt going into cluster formation the DMS FM glue may be too weak or absent in this case. It may also be interesting to consider whether and how dilutely embedded magnetic clusters could magnetically interact in a conducting or semiconducting matrix via carriers

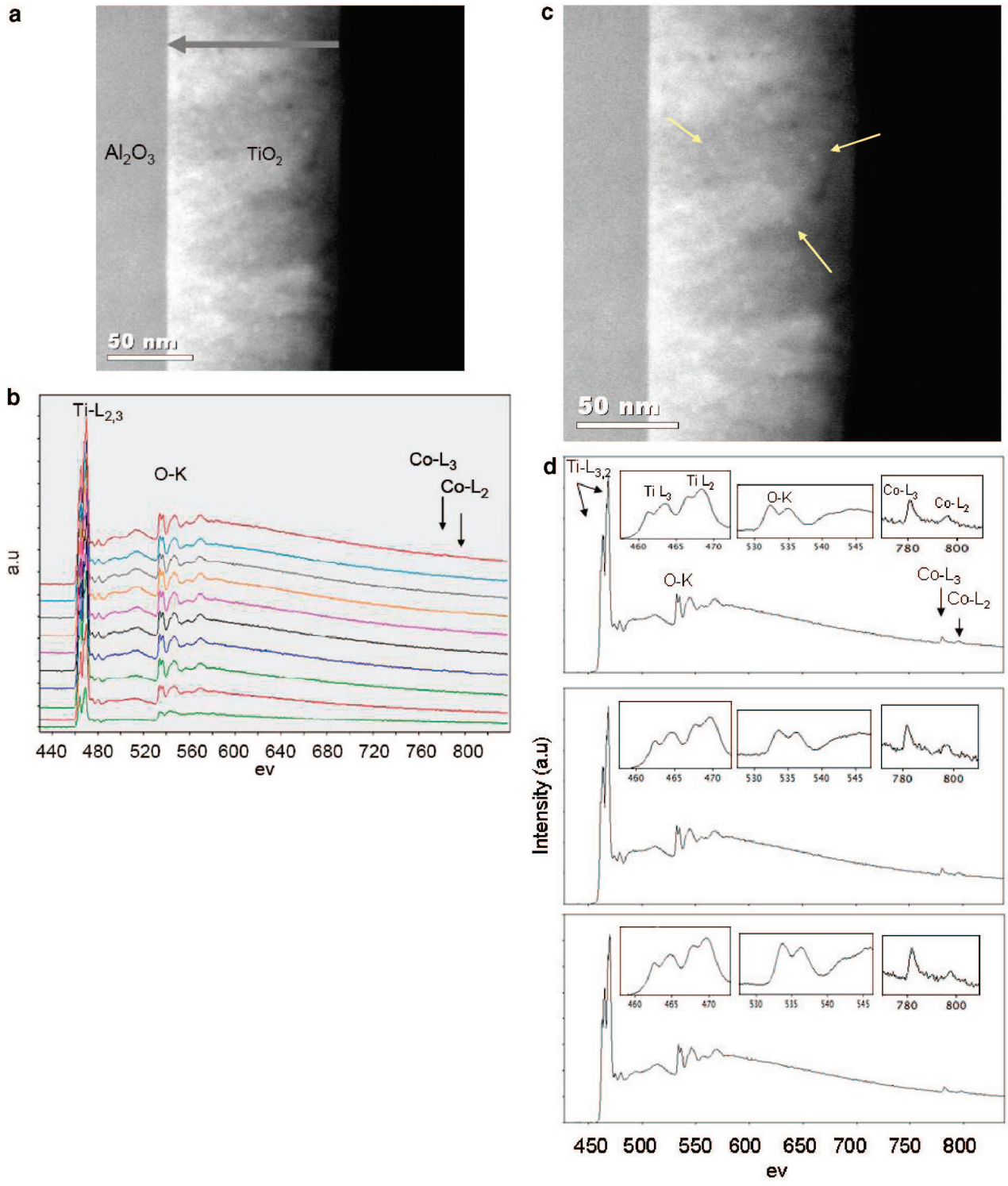

Figure 6. (a) High-resolution cross-section HAADF STEM data for the $Co_{0.04}Ti_{0.96}O_2$ film grown at 400 °C at 100 mTorr of Ar + H_2. (b) EELS data recorded at various points across the film cross-section. (c) Same image as in image a, showing the locations by arrows where the EELS in (d were recorded. (d) EELS data recorded at three specific points exhibiting brighter contrast in the HAADF image indicated in image c. The insets show the details.

or polarons.[11–19] Another possibility is that the type of clusters in the vacuum-grown case and Ar + H_2 grown case are different and the strength of the corresponding FM is different. As will be discussed later, the degree of anion (oxygen) poor character of growth environment can change the extent of substitutional cobalt incorporation, associations, interestial cobalt concentrations, oxygen vacancy defects, etc., and these collectively define magnetism, including saturation moment.

In panels a and b in Figure 8, we compare the XAS and XMCD data, respectively, for the $Co_{0.04}Ti_{0.96}O_2$ film grown at 400 °C and 100 mTorr of Ar + H_2 and in a vacuum, once again remembering that these data correspond only to the top 5–10 nm thickness of the film. It is clear that in both cases the XAS signal shows the Co^{2+} type L-edge fine structure, whereas the corresponding fine structure in XMCD appears somewhat well-developed only in the case of the Ar + H_2 grown film.

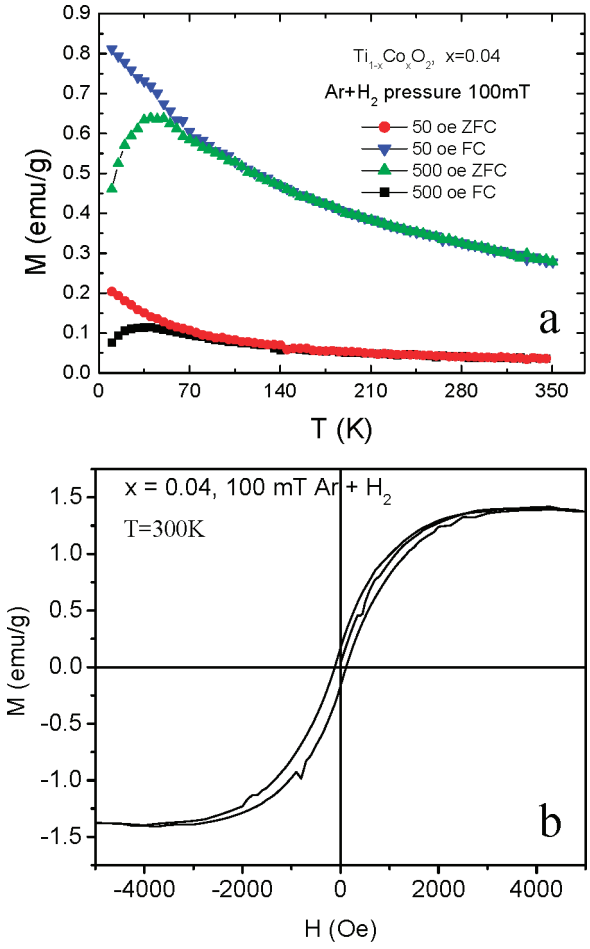

Figure 7. Field-cooled and zero-field-cooled magnetization of a $Co_{0.04}Ti_{0.96}O_2$ film grown at 400 °C and 100 mTorr of Ar + H_2. (b) Room-temperature $M-H$ loop for the same case.

This is rather surprising and suggests that the charge sharing near the surface has other contributions. Hence, we looked at the Ti XAS signal, which is shown in Figure 9. It can be easily seen that the signal shows significant departure only for the case of film grown in Ar + H_2. We found that this sample had golden color (like TiN), possibly suggesting the Ti^{3+} state. This is remarkable in light of the recent suggestion by Dietl and co-workers[42] that valence control could be used to manipulate and control dopant clustering and self-assembly of nanodots. What we show is that growth in hydrogen atmosphere may be an interesting approach to achieve both these objectives.

Finally, it is useful to compare the temperature dependence of low field magnetization between the two cases of films grown in a vacuum and in Ar + H_2 atmosphere for x = 0.04 (Figures 3b and 7a). Within the molecular field theory approximation,[44] the magnetization of a magnetic cluster system can be written as

$$M(T,H) = Nm(T)L\{m(T)(H + \alpha M(T,H))((k_BT)\}; m(T) = m(0)f(T/T_c^{\text{cluster}})$$

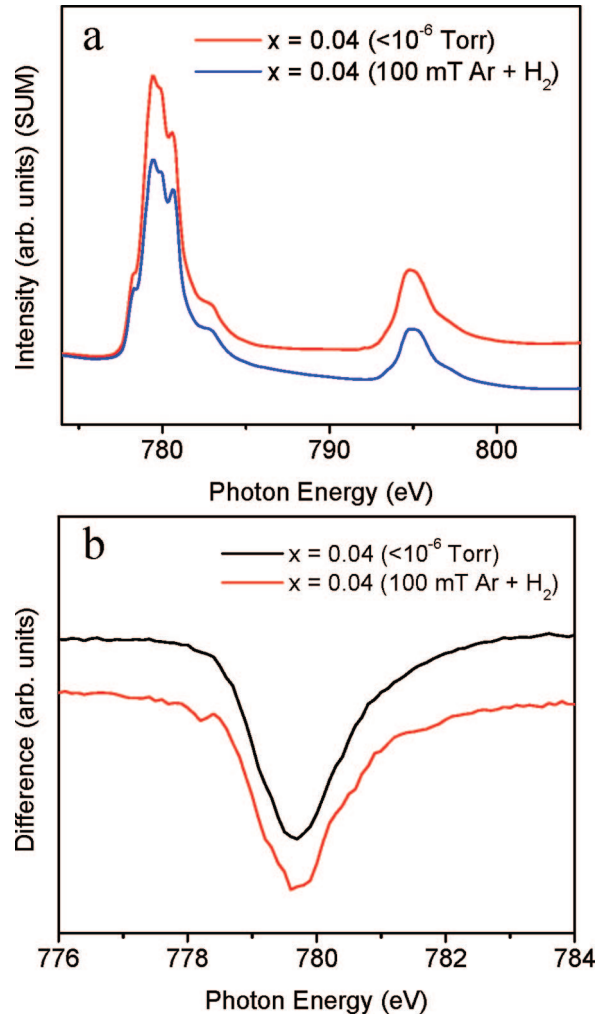

Figure 8. Comparison of the (a) X-ray absorption and (b) X-ray magnetic circular dichroism data for the $Co_{0.04}Ti_{0.96}O_2$ film grown at 400 °C and 100 mTorr of Ar + H_2, and in a vacuum greater than 1 × 10^{-6} Torr.

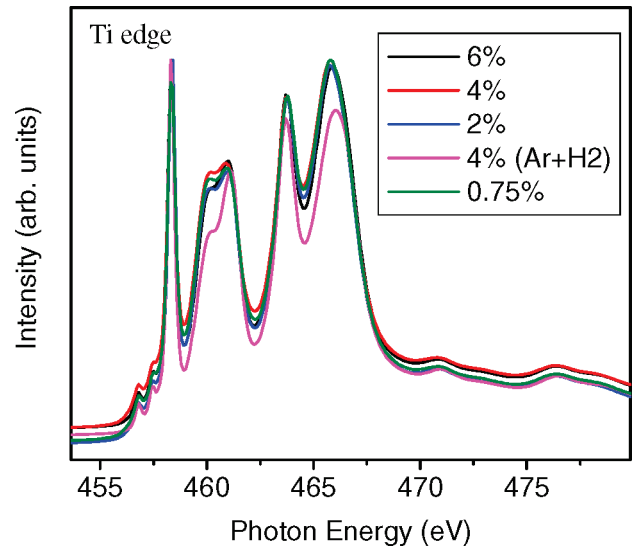

Figure 9. X-ray absorption data corresponding to Ti edge for thin film samples grown under different conditions.

where L is the Langevin function, N is the number of clusters in a unit volume of the sample, $m(T)$ is the average magnetic moment of a magnetic cluster at temperature T, α is the molecular field parameter and defines the interaction

(44) Wang, L.; Ding, J.; Li, Y.; Feng, Y. P.; Phuc, N. X.; Dan, N. H. *J. Magn. Magn. Mater.* **2001**, *226–230*, 1504. J. Appl. Phys. 2001, 89, 8046.

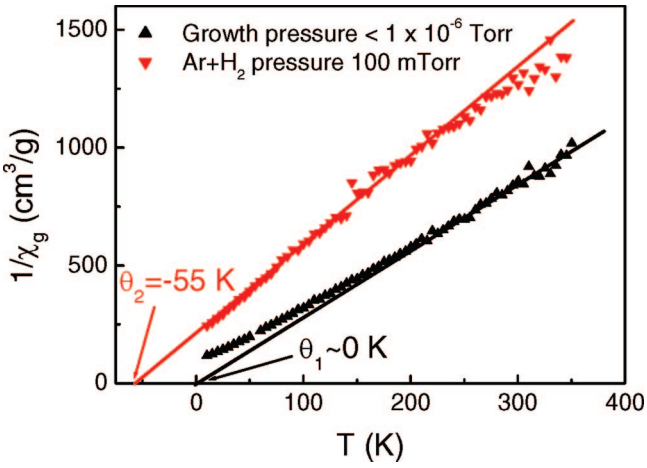

Figure 10. Comparison of $1/\chi$ (inverse magnetic susceptibility) dependence on temperature for the $Co_{0.04}Ti_{0.96}O_2$ film grown at 400 °C and 100 mTorr of Ar + H_2, and in a vacuum greater than 1×10^{-6} Torr.

between clusters, $T_c^{cluster}$ is the Curie temperature of the magnetic cluster, when $T \ll T_c^{cluster}$, $f(T/T_c^{cluster}) \approx 1$. In our cobalt cluster system, $T_c^{cluster} \approx 1400$ K, and the temperature we are considering is below 350 K, so we can approximately have $m(T) \approx m(0)$: the saturation magnetization of the single domain size cluster.

And as $L(x \ll 1)$ is $\sim x/3$, in the low magnetic field range (in our case, $H = 50$ oe), we can have

$$M(T,H) = Nm(0)^2(H + \alpha M(T,H))/3k_BT$$

Then we can have the susceptibility as

$$\chi = M/H = Nm(0)^2/2k_B(T-\theta)$$

where $\theta = N\alpha m(0)^2/3k_B$ defines the interaction between clusters. We can plot $1/\chi$ vs T and the extrapolation gives rise to the temperature θ.

As shown in Figure 10, we obtain $\theta_1 \approx 0$ K, $\theta_2 \approx -55$K for the high-vacuum-deposited sample and the Ar + H_2 one, respectively.

The $\theta_2 \approx -55$K suggests antiferromagnetic interaction between clusters in the sample deposited in Ar/H_2. Very interestingly, the $1/\chi$ vs T curve for high-vacuum sample tilts upward at low temperatures, which indicates concurrent existence of the FM phase with Curie temperature lower than room temeprature. Instead of a positive extrapolated temperature for the pure FM phase, θ is found to be ~ 0 K, which suggests a competition between the intrinsic DMS FM phase and AFM coupling between clusters. This may also explain the higher magnetization (lower $1/\chi$) in the high-vacuum-grown sample than that in the Ar/H_2-grown sample.

There have been theoretical and computational studies which collectively suggest that the electrical and magnetic properties of the $Co:TiO_2$ system should be fairly sensitive to the growth conditions as observed here. Sullivan and Erwin[45] have reported first-principles microscopic calculations of the formation energy, electrical activity, and magnetic moment of Co dopants and a variety of native defects in anatase TiO_2. Using these results and equilibrium thermodynamics they find that under commonly employed O-poor growth conditions a substantial fraction of Co dopants occupies interstitial sites as donors, which due to incomplete compensation by substitutional Co acceptors lead to n-type behavior. Geng and Kim[46] have reported on the interplay between local structure and magnetism in anatase $Co:TiO_2$ based on ab initio density-functional calculations. Their calculated formation energy of a pair of substitutional Co ions indicates that they have a tendency to cluster without noticeable effect on the low-spin state of Co. This is different than a cobalt metal (Co(0)) cluster. Further, they find that the interstitial Co is strongly attracted to a substitutional Co; in fact, more strongly to a substitutional Co pair. Whereas magnetism is enhanced for the former situation, it is destroyed for the latter. These results are consistent with the strong sample-to-sample variability of the magnetic moment of Co in experiments. Recently, Janisch and Spaldin[47] have performed first-principles computational study of the Co-doped TiO_2 system. They have calculated the magnetic ordering and electronic properties as a function of the Co concentration and distribution of Co dopants and oxygen vacancies. They find that Co atoms prefer to substitute on neighboring sites of the Ti lattice and, importantly, this leads to a ferromagnetic superexchange. Zunger[48] has laid out some practical doping principles for oxide matrices. He suggests that the enthalpy of forming anion vacancies decreases under host cation-rich conditions, whereas the enthalpy of forming cation vacancies decreases under host anion-rich conditions. He further suggests that cation-substituting dopants should be more soluble under host-cation poor (= host-anion rich) growth conditions. All these works collectively point to a close and rather sensitive connection between the dopant location, defects, the precise nature of the microstate, and the magnetic/electrical properties of the system. Our results demonstrate that this interplay plays out even at a low growth temperature of 400 °C as the ambient conditions are changed, implying that the different microstates are separated by only small energy scales.

In conclusion, we have examined the properties of diluted magnetic semiconductor $Co:TiO_2$ in thin films grown at relatively low temperature of 400 °C in different reducing ambients. We have studied the evolution of the microstate carefully using finer elemental probes and have concurrently examined the magnetic properties. It appears that the $Co:TiO_2$ system is susceptible to the formation of tiny cobalt associations within the matrix (not necessarily metal clusters) even at low temperature beyond some level of solubility (uniform distribution). This suggests a mixed-state scenario for ferromagnetism in this system. We have also shown that growth under controlled ambient (Ar + H_2) can lead to a fairly uniform magnetic nanodot assembly across the film cross section, the formation of which appears to be driven by matrix cation valence control.[42]

(45) Sullivan, J. M.; Erwin, S. C. *Phys. Rev. B* **2003**, *67*, 144415.
(46) Geng, W. T.; Kim, K. S. *Solid State Commun.* **2004**, *129*, 741.
(47) Janisch, R.; Spaldin, N. A. *Phys. Rev. B* **2006**, *73*, 035201.
(48) Zunger, A. *Appl. Phys. Lett.* **2003**, *83*, 57.

Acknowledgment. S.B.O. thanks BRNS (DAE, Government of India) for a research grant under CRP in spintronics and the Department of Science and Technology (DST) for the award of Ramanujan Fellowship. T.V. acknowledges support from DARPA (ONR), Grant N000140210962. N.B. acknowledges support from DOE Contract DE-AC02-05CH11231 and NSF Grant DMR-0335364. Idzerda acknowledges ONR Grant N00014-03-01-0692d and DARPAs Grant N000140210962d.

Supporting Information Available: STEM image and line scane for a highly milled 4% Co:TiO_2 film sample (PDF). This material is available free of charge via Internet at http://pubs.acs.org.

CM702089Z